Design of deterministic light-trapping structures for thin silicon heterojunction solar cells

SAMIA AHMED NADI,[1] KARSTEN BITTKAU[1,*], FLORIAN LENTZ,[1,2,] KAINING DING,[1] AND UWE RAU[1]

[1] *IEK5- Photovoltaic, Forschungszentrum Jülich GmbH, 52425 Jülich, Germany*
[2] *Currently with Helmholtz Nano Facility (HNF), Forschungszentrum Jülich GmbH, 52425 Jülich, Germany*
**k.bittkau@fz-juelich.de*

Abstract: We optically designed and investigated two deterministic light-trapping concepts named "Hutong" (wafer thickness dependent, patch-like arrangement of "V" grooves with alternating orientations) and "VOSTBAT" (one directional "V" grooves at the front and saw-tooth like structures at the back) for the application in emerging thin silicon heterojunction (SHJ) solar cells. Calculated photocurrent density (J_{ph}) (by weighting the spectrally resolved absorptance with AM1.5g spectrum and integrating over the wavelength) showed that both Hutong and "VOSTBAT" structures exceed the Lambertian reference and achieved J_{ph} of 41.72 mA/cm^2 and 41.86 mA/cm^2 respectively on 60 µm thin wafer in case of directional, normal incidence.

1. Introduction

At present, crystalline silicon (c-Si) based solar cells and modules are the leading technology for the photovoltaic (PV) industry with a market share of about 95% [1]. But due to the indirect band gap of c-Si and, therefore, weak absorption of photons with energies close to the band gap energy, solar cells with c-Si absorber layers are often around 180-200 µm thick to ensure adequate absorption of sunlight. Thin Si wafers, produced either by thinning or kerfless wafering techniques, are promising buildings blocks for low cost and high efficiency Si photovoltaics. Several researches have proven that absorber layer thinning can minimize recombination rates due to intrinsic Auger recombination processes and hence, lead to maximum possible open-circuit voltage (V_{oc}) [2-4]. Silicon heterojunction (SHJ) concept is among the highest efficiency c-Si solar cells due to the high V_{oc} values enabled by the excellent passivation quality of c-Si surface [5]. One of key advantages of this technology is the low processing temperature (<200 □C) [5] which qualifies the use of ultra-thin wafers without triggering any substrate deformation.

Although thinner wafers allow for better material flexibility and higher open-circuit voltages, their photocurrents are reduced due to the weak absorption of long wavelength radiation. This issue can be overcome by using tailored light management concepts such as texturing of Si wafers [6]. Surface texturing of c-Si improves the anti-reflection properties for light of shorter wavelengths and elongates the path length of light with longer wavelengths inside the Si absorber [7-9]. Various photonic light-trapping concepts have been researched, such as: nano-wires [10-11], nano-cones and domes [12-13], nano-cylinders [14], periodic inverted nano-pyramids etc. [15-16]. These micro-/nano-structures have excellent light-trapping capabilities but complex and often expensive fabrication processes. They can show high surface recombination due to increased surface area, sharp edges or plasma damage [17-18], leading to reduced conversion efficiencies. Therefore, applying advanced light-trapping

structures with minimal sharp edges and extended facets on the emerging ultra-thin c-Si wafers can pave the way towards high efficiency and cost competitive ultra-thin SHJ solar cells.

Light-trapping with "patch textures" featuring defined facet orientations have shown excellent light-trapping properties [19-21]. Thorstensen et al. have produced such patch textures by laser assisted texturing and compared their result with ray-tracing simulations [22]. In this work, we investigated two deterministic light-trapping structures. The first structure is called "Hutong" (inspired by the architecture of traditional rooftops of Hutong houses in Beijing) based on the "single-sided patch texture" from Campbell et al. [19], which is basically parallel "V-shaped" grooves processed in a patch similar to a checkerboard layout as shown in Fig. 1(a) and Fig. 1(c). Each patch has parallel "V-shaped" grooves along one direction and each directly adjacent patch shows parallel "V-shaped" grooves oriented along the perpendicular direction. The patch size highly depends on the wafer thickness. Here reported "Hutong" structure is expected to provide an outstanding optical performance especially for thin PV devices by almost fully trapping the light for the first six passes through the Si absorber layer.

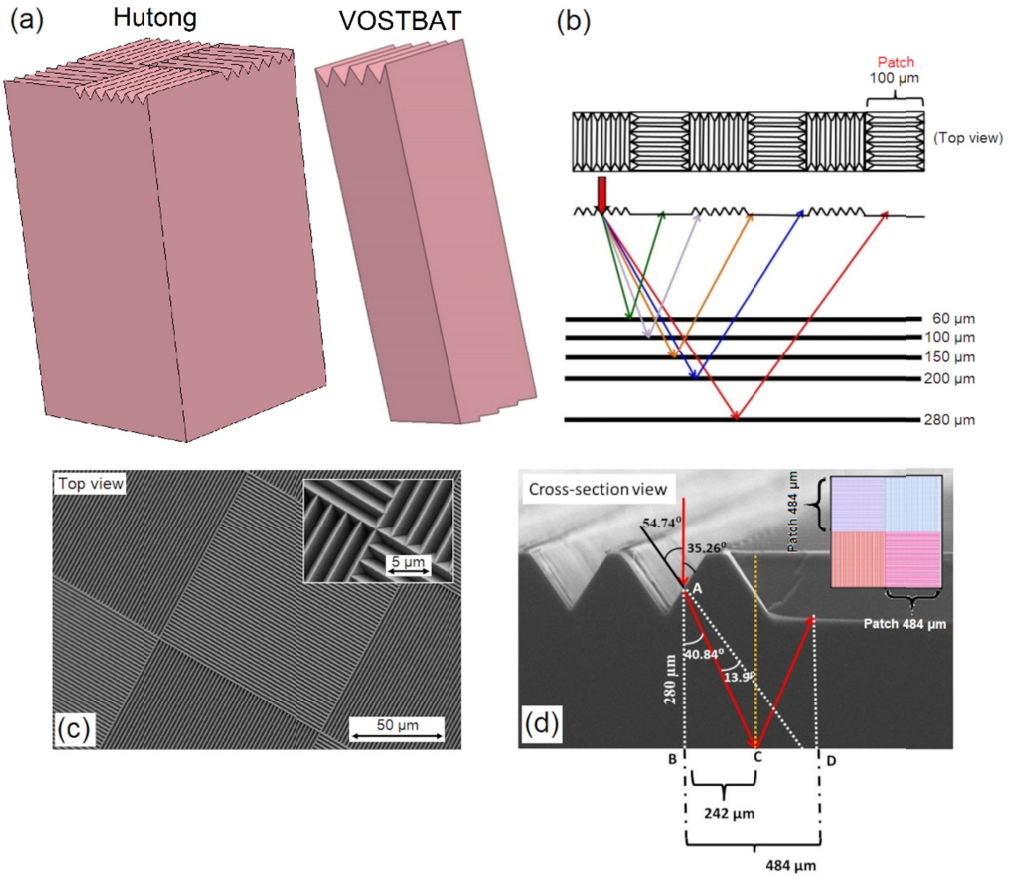

Fig. 1. (a) 3D sketch of the Hutong and VOSTBAT structures, (b) Hutong structure on different wafer thicknesses, (c) fabricated Hutong structure on a 280 µm c-Si wafer with 100 µm patch size, (d) working principal of Hutong structure

The second structure is called "VOSTBAT" (V-grooves On Saw Tooth BAck side Texture). This structure was inspired by "double-sided perpendicularly grooved texture" of Campbell et al. [18] where instead of the perpendicular grooves at the bottom, we utilized an asymmetric saw-tooth like shape for better determination of the light path.

Both structures profit from the fact that at least for the first passes through the wafer, the light can only couple into well-defined modes, instead of being randomized. Therefore, effective light path enhancements beyond that for the fully randomizing Lambertian reference are in principle possible in a broad spectral range.

In this work, we evaluated the optical effects of Hutong and "VOSTBAT" for different patch sizes according to different Si wafer thicknesses and different angles of saw tooth structure, respectively. The simulation work was performed by using the ray-tracing module of the simulation software "Sentaurus Device" [23] to understand the effect of deterministic light trapping structures. These results were compared with simulation results of 2 μm regular periodic inverted pyramids (PIP) and 2 μm random pyramids. The results for the PIP structure were obtained from PV Lighthouse ray tracing tool [24].

2. Deterministic light-trapping structures for thin Si absorber

2.1 Hutong

The Hutong structure is basically "V" grooves patterned in column-row-column structure as shown by the SEM image in Fig. 1(c). The aim of Hutong structure is to make sure that while the incident light (especially infrared light) refracts into the thin Si wafer through a "V" groove of columnar facet with a well-defined angle, it travels all the way to the bottom of the Si wafer. While it reaches the Si bottom, the ray will reflect back towards the front. But when the ray reaches the front, it will face a different "V" groove of row facet, therefore, it will reflect back into the absorber because the angle of incidence is always larger than the critical angle for total internal reflection.

To make sure that when the light tries to escape from the front, it intersects at a different facet than its incident facet, patch sizes were calculated according to their wafer thickness following Snell's law. As shown in Fig. 1(d), if the wafer thickness is 280 μm, for the incident light to hit the back side and reach the front, it will intersect the front interface 484 μm away from the first intersection. Therefore, the optimal patch size is 484 μm. Different wafer thicknesses provide different optimum patch sizes as shown in Fig. 1(b).

2.2 VOSTBAT (V-grooves On Saw Tooth BAck side Texture)

The VOSTBAT structure mainly achieves the deterministic light trapping by the back-side texture. Due to utilizing a saw-tooth like pattern, as shown in Fig. 1(a), the internal angle of the light is increased immensely subsequently with each reflection at the back side. Although this already provides a deterministic light-trapping scheme, similar to the suggestion by Rau et al. [25], the front side is additionally textured in a way that does not conflict with the deterministic approach of the back-side texture. This is assured by the different orientation of the "V" grooves at the front side compared to the saw tooth structure at the back side. Thereby, the elongation of light paths is happening along independent axes. Furthermore, the front side texture allows for a significantly lower primary reflectance compared to a flat front side. As the most important parameter of the VOSTBAT structure is the angle of the saw tooth structure, determining this angle is the most significant part in this research.

A possible approach to fabricate such a back-side structure may include a "post passivation light trapping back contact", as demonstrated by Smeets et al. [26].

3. Simulation results on thin Si wafer

3.1 Hutong

To investigate the optical advancement of the advanced light-trapping structures, the commercial tool Sentaurus TCAD by Synopsis was used as it allows creating deterministic 3D structures easily with the Sentaurus Structure Editor module. From the structure, an adapted mesh was generated which was used as input for the optical simulation. Since all geometrical structures had sizes significantly larger than the wavelength of light, the ray-

tracer of Sentaurus Device module was used for the calculation of the reflectance. According to the calculation following Snell's law, for 60 µm thin wafers, required patch size for Hutong is 104 µm whereas VOSTBAT structure is independent from the wafer thickness.

By weighting the spectrally resolved 1-reflectance (1-R) with the AM1.5g spectrum and integrating over the wavelength, the results were transformed to a photocurrent density (J_{ph}), which provides a much more relevant property for the application in solar cell devices. The application of anti-reflection coating (ARC) is necessary to separate light-trapping properties from light incoupling. Therefore, simulations were performed with PV Lighthouse on 2 µm regular PIP with 100% area filling (AF) to find the optimal thickness for ITO. The optical data for ITO was taken from literature [27]. ITO thickness of 68 nm was found to show the best anti-reflection properties. As the facet angles were identical for 2 µm regular PIP and Hutong structure, the same ITO thickness was used for Hutong structure.

In an ideal deterministic light trapping structure, the light path is well defined for the whole multiple passes through the wafer [25]. In case of our Hutong structure, the patch size is adapted to the refraction angle of incident light when passing from air through the front interface. After the light passed forth and back through the wafer, it hits the front interface at a patch with opposite orientation of the V-grooves, thereby it is always totally internally reflected. Due to the geometrical structure, the angle of that reflected light has a different angle than at the first pass. Therefore, the patch size is not perfectly adapted to this. This is limiting the advantage of the deterministic light trapping concept, leading to losses after the fourth pass depending on the position of the light ray. Furthermore, this leads to the fact that a local maximum of optical properties was demonstrated by 92 µm patch size, instead of calculated 104 µm patch size, since this patch size is a better compromise when considering not only the first and second pass through the wafer.

It has to be noted that the Hutong concept is also working for significantly lower patch sizes. As illustrated in Fig. 1(b), an incident light ray, which is refracted by the "V" grooves at the front interface, might skip patches at the front interface after reflection at the back side. As long as the light ray hits the front interface at a patch with perpendicular orientation of the "V" grooves, the functionality should be the same. Hence, we investigated different smaller patch sizes with different number of "V" grooves within each patch. We found the highest optical performance for a patch size of 35.5 µm with 16 "V" grooves per patch.

3.2 VOSTBAT

Sentaurus TCAD tool was also used to investigate the optical properties of VOSTBAT structure. Unlike Hutong, VOSTBAT is not thickness dependent. Hence, different angles (7-10□) of the saw tooth structure as well as the number of "V" grooves and saw tooth structures inside one spatial domain were varied in this work. The spatial domain size was chosen to be 35.5x35.5 µm² to be in alignment with the optimal Hutong structure. The numbers of "V" grooves and saw tooth structures were kept equal. The optimal number of "V" grooves and saw tooth structures was found to be four. This leads to a lateral period of 8.875 µm at the front and back interface. The optimal angle of the saw tooth was found to be 8°. The absorptance in 60 µm thin c-Si wafer with ITO front layer and optimized VOSTBAT structure exceeded those for both Hutong and the reference value that is given by the maximum randomization of the light that is penetrating into the solar cell (Lambertian reference). The results will be shown in the following section in comparison to the other investigated structures.

4. Comparison of all the light-trapping structures

Hutong of 92 µm and 35.5 µm patch, the optimized VOSTBAT structure, 2 µm regular PIPs and random pyramids were compared with the Lambertian reference, as calculated by M. A. Green [8]. To compare the acquired results with the Lambertian reference, the absorptance results were normalized at 950 nm wavelength (internal absorptance A'), since Lambertian

reference assumes the incident light is perfectly coupled into the absorber unlike ray tracing simulation. At that wavelength, the absorptance of incident light is almost the same for all light trapping structures, which means that the light is fully absorbed even without light scattering. Furthermore, the wavelength of 950 nm is spectrally close enough to the relevant range for light trapping that the anti-reflection properties of the front ITO layer are quite similar. Figures 2(a) and 2(b) show normalized (internal) and not normalized (external) absorptance of all the light-trapping structures against wavelength and thickness corrected absorption coefficient (αw), respectively. In both cases, it is clearly visible that optimized VOSTBAT and Hutong both show significantly higher internal (Fig. 2(a)) and external (Fig. 2(b)) absorptance than the Lambertian reference in a wide spectral range. As one can see, 2 µm regular PIP, 2 µm random upright pyramids (URP) both with both sides textured and flat back side show a lower absorptance than Lambertian reference in the whole spectral range (Fig. 2(a)).

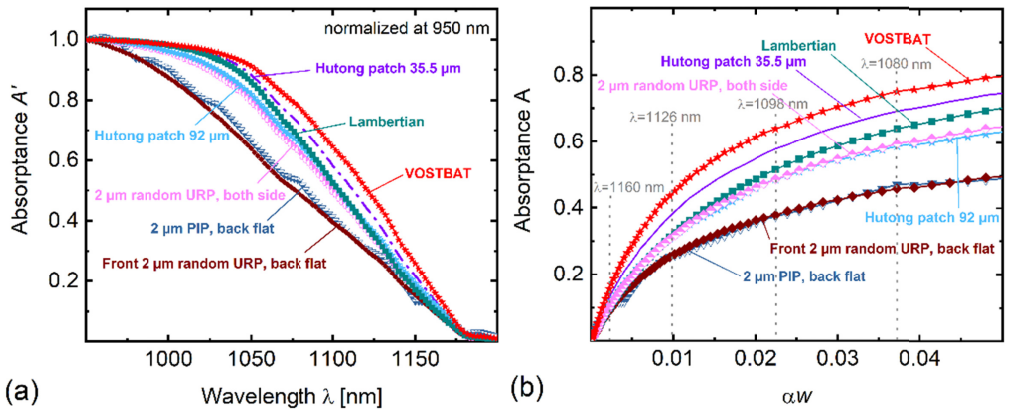

Fig. 2. (a) Internal absorptance of different light trapping structures as a function of the wavelength, (b) external absorptance of different light trapping structures as a function of thickness corrected absorption coefficient (αw), where w is 60 µm, the thickness of Si wafer and α is the wavelength dependent absorption coefficient.

By weighting the internal absorptance with the AM1.5g spectrum and integrating over the wavelength, the results were transformed to a photocurrent density (J_{ph}) which showed that in the long wavelength range (950-1200 nm), Hutong of 35.5 µm patch and VOSTBAT structure outperformed Lambertian scatterer depicting $J_{ph,950\text{-}1200nm}$ of 7.50 mA/cm2 and 7.72 mA/cm2, respectively, compared to Lambertian reference of 7.285mA/cm2 (Fig. 3(a)).The results were compared to different pyramid-based structures. Taking the spectral range from 950-1200 nm into account, all structures with pyramids and Hutong with bigger (92 µm) patch size generated a $J_{ph,950\text{-}1200nm}$ lower than for the Lambertian reference (Fig. 3(a)).

Figure 3(b) shows the internal effective path length in units of the wafer thickness, calculated as $\frac{l_{eff}}{w} = -\frac{1}{\alpha w}\ln(1-A')$. It can be seen that, due to the deterministic light-trapping scheme [25], the effective path length, l_{eff} was longest for VOSTBAT, followed by the Hutong structure with 35.5 µm patch size. The only other structure that overcame Lambertian reference was Hutong with 92 µm patch from 1115 nm wavelength onwards. The 2 µm PIP structure showed a resonant feature at wavelengths 1140nm-1175nm, partly exceeding the Lambertian reference. The effective path length for the random URP with both sides textured was also slightly longer than for the Lambertian case. Both was explained by resonant effects for the specific representation of the structure as well as the light source, where well-defined positions for the incident light rays were assumed.

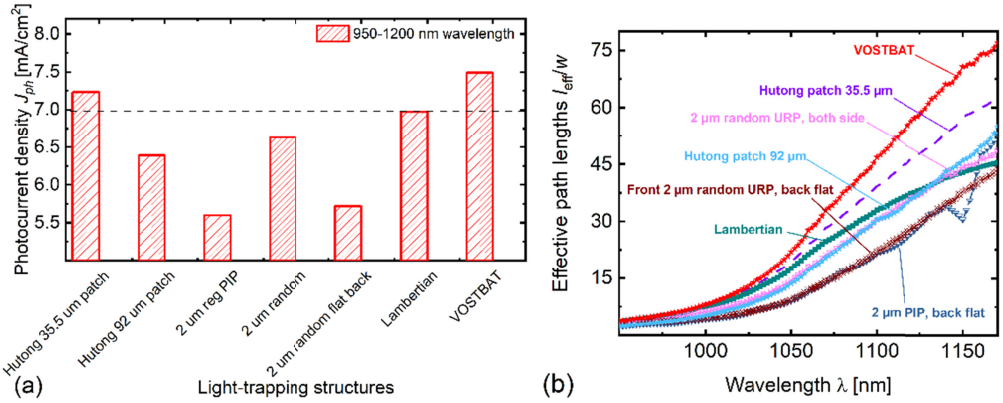

Fig. 3. (a) Acquired internal photocurrent density of different light trapping structure in the long wavelength range (950 – 1200 nm), (b) Relative path lengths (l_{eff}/w) of different light-trapping structures as a function of wavelength.

An alternative quantity to evaluate the light-trapping properties was introduced as a figure of merit (FOM_{RPK}) by Rau et al. [25], which is the inverse expectation value of the distribution of the reciprocal path lengths: $FOM_{RPK} =< 1/l >^{-1} = \int 1 - A'(\alpha) d\alpha$. This figure of merit was calculated for the different structures and normalized with the wafer thickness and is shown in Fig. 4.

It can be seen from Fig. 4 that the VOSTBAT structure as well as the Hutong structure with 35.5 µm patch size show a FOM_{RPK} above the Lambertian reference. All other investigated structures had a lower FOM_{RPK}. Therefore, it can be stated that Fig. 3(b) and Fig. 4, both are in good agreement proving the performance of deterministic light-trapping structure.

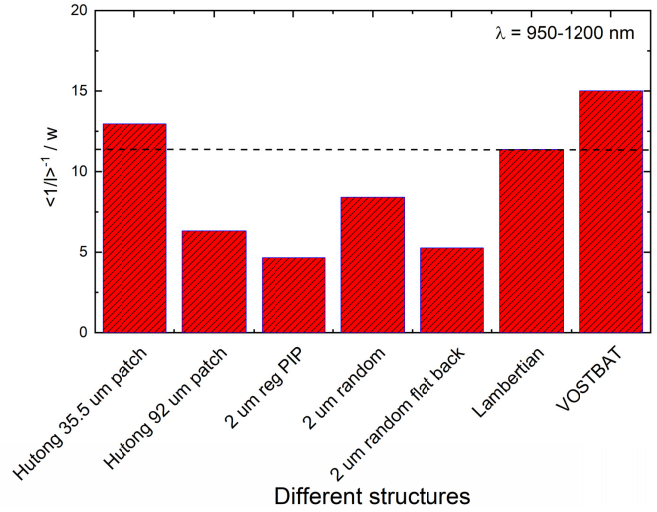

Fig. 4. Figure of merit $<1/l>^{-1}/w$ of different light-trapping structures.

Fig. 5(a) shows the ratio of normalized absorptance between the deterministic light-trapping structures compared to the Lambertian reference. It can be seen that with increasing wavelength, the absorptance for both structures increased significantly. At a wavelength of 1150 nm, the Hutong structure with 35.5 µm patch size and the VOSTBAT structure showed an absorptance that is 28% and 53% above the Lambertian reference, respectively. In order to evaluate our deterministic light-trapping structures for a more realistic application, we plotted

the external absorptance, i.e. the amount of generated electron-hole pairs inside the c-Si wafer per incident photon, in the spectral range from 300 nm to 1200 nm in Fig. 5(b). We compared the results to a modified Lambertian reference by multiplying the Lambertian reference with the front layer transmission. Thereby, all primary reflection at the front interface was considered. In the spectral range from 300 nm to 950 nm, all absorptance curves look the same as only the front layer transmission determines the absorptance in the wafer due to the high absorption coefficient of c-Si in that range. Differences can only be seen from 950 nm to 1200 nm with the VOSTBAT structure showing the highest and the Lambertian reference showing the lowest values. The related photocurrent density was calculated by multiplying the absorptance with the AM1.5g spectrum and integrating over the wavelength. The values are shown in the labels. The highest photocurrent density J_{ph} achieved at this work was 41.86 mA/cm2 by the VOSTBAT structure followed by the Hutong structure with 35.5 µm patch size (41.72 mA/cm²). In the case of the modified Lambertian reference, a value of 41.44 mA/cm² was achieved. Note, that we assumed an ITO layer with realistic absorption properties, but we neglected passivation and doping layers in our study.

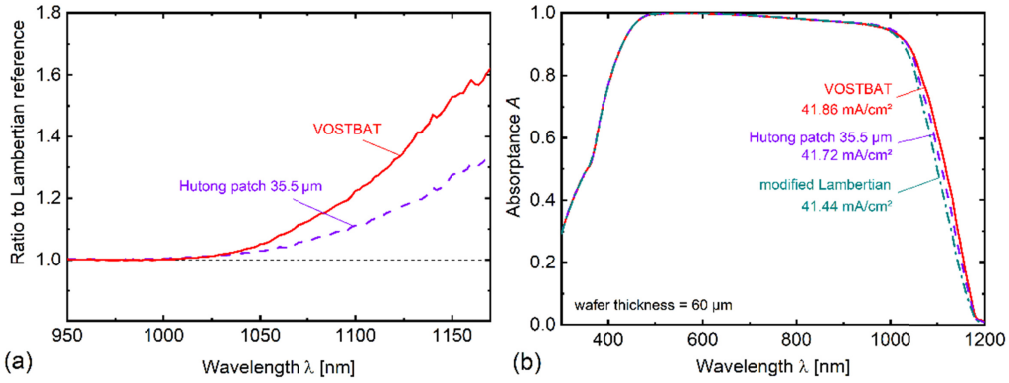

Fig. 5. (a) Ratio of the normalized absorptance of our deterministic light-trapping structures to the Lambertian reference. (b) Absorptance spectra of the light-trapping structures and acquired photocurrent density.

In case of a realistic application, it has to be considered that the presented light-trapping concept requires a tracking system to ensure the normal incidence of sunlight. Furthermore, the patch size of the Hutong structure as well as the angle of the saw tooth in the VOSTBAT structure for a solar module must be adapted to the refractive index of the encapsulation material to achieve the same functionality. During processing, special care must be taken to keep the flat areas at the tip of the ridges as small as possible, as this could reduce light-trapping performance.

5. Conclusion

Both deterministic light-trapping structures Hutong and VOSTBAT demonstrated excellent light-trapping properties and exceeded the Lambertian reference by 0.28 mA/cm² and 0.42 mA/cm², respectively, in the full spectral range for directional illumination at normal incidence. These structures were well investigated by optical simulation to be implemented on ultra-thin and/or kerfless wafer technology. The Hutong structure consisted of a patch pattern with "V" grooves of different orientation. The size of the pattern was adapted to the wafer thickness to increase the effective light path in the solar cell absorber. Optical simulation results showed that Hutong and VOSTBAT both structures outperformed not only the Lambertian reference but also the popular pyramid textures. The VOSTBAT structure demonstrated the best optical properties among all the mentioned light-trapping structures depicting $J_{ph,950\text{-}1200nm}$ of 7.72 mA/cm2 in the long wavelength range.

Funding

HITEC Graduate School; Helmholtz Energy Materials Foundry; European Commission Horizon 2020 Program for research, technological development and demonstration (Grant No. 727523).

Disclosures

The authors declare that there are no conflicts of interest related to this article.

References

1. SEMI, International Technology Roadmap for Photovoltaic (ITRPV), 11th ed. <https://itrpv.vdma.org/download> (accessed: May, 2020).
2. M. A. Green, "Limits on the open-circuit voltage and efficiency of silicon solar cells imposed by intrinsic Auger processes," IEEE Trans. Electron Devices **ED-31**, 671 (1984).
3. T. Tiedje, E. Yablonovitch, G. D. Cody, and B. G. Brooks, "Limiting efficiency of silicon solar cells," IEEE Trans. Electron Devices **ED- 31**, 711 (1984).
4. A. Bozzola, P. Kowalczewski, and L. C. Andreani, "Towards high efficiency thin-film crystalline silicon solar cells: The roles of light trapping and non-radiative recombinations," J. Appl. Phys. **115**, 094501 (2014).
5. S. De Wolf, A. Descoeudres, Z. C. Holman, and C. Ballif, "High-efficiency Silicon Heterojunction Solar Cells: A Review," Green, **2**(1), 7-24 (2012).
6. E. Yablonovitch, and G. D. Cody, "Intensity enhancement in textured optical sheets for solar cells," IEEE Trans. Electron. Dev. **29**(2), 300–305 (1982).
7. D. Redfield, "Multiple-pass thin-film silicon solar cell," Appl. Phys. Lett. **25**, 647 (1974).
8. M. A. Green, "Lambertian light trapping in textured solar cells and light-emitting diodes: Analytical solutions," Prog. Photovolt. Res. Appl. **10**(4), 235–241 (2002).
9. E. Yablonovitch, "Statistical ray optics," J. Opt. Soc. Am. **72**(7), 899–907 (1982).
10. E. Garnett, P. Yang, "Light Trapping in Silicon Nanowire Solar Cells," Nano Lett. **10**, 1082 (2010).
11. M. D. Kelzenberg, S. W. Boettcher, J. A. Petykiewicz, D. B. Turner-Evans, M. C. Putnam, E. L. Warren, J. M. Spurgeon, R. M. Briggs, N. S. Lewis, H. A. Atwater, "Enhanced absorption and carrier collection in Si wire arrays for photovoltaic applications," Nat. Mater. **9**, 239 (2010).
12. R. Khandelwal, U. Plachetka, B. Min, C. Moorman, H. A. Kurz, "A comparative study based on optical and electrical performance of micro- and nano-textured surfaces for silicon solar cells," Microelectron. Eng. **111**, 220 (2013).
13. Y. M. Song, J. S. Yu, Y. T. Lee, "Antireflective submicrometer gratings on thin-film silicon solar cells for light-absorption enhancement," Opt. Lett. **35**, 276 (2010).
14. K. J. Yu, L. Gao, J. S. Park, Y. R. Lee, C. J. Corcoran, R. G. Nuzzo, D. Chanda, J. A. Rogers, "Light Trapping in Ultrathin Monocrystalline Silicon Solar Cells," Adv. Energy Mater. **3**, 1401, (2013).
15. A. Mavrokefalos, S. E. Han, S. Yerci, M. S. Branham, G. Chen, "Efficient Light Trapping in Inverted Nanopyramid Thin Crystalline Silicon Membranes for Solar Cell Applications," Nano Lett. **12**, 2792, (2012).
16. M. S. Branham, W.-C. Hsu, S. Yerci, J. Loomis, S. V. Boriskina, B. R. Hoard, S. E. Han, A. Ebong, and G. Chen, "Empirical Comparison of Random and Periodic Surface Light-Trapping Structures for Ultrathin Silicon Photovoltaics," Advanced Optical Materials **4**, 858–863 (2016).
17. S. Sivasubramaniam, M. M. Alkaisi "Inverted nanopyramid texturing for silicon solar cells using interference lithography," Microelectronic Engineering **119**, 146-150 (2014).
18. I. Abdo, C. Trompoukis, L. Tous, V. Depauw, R. Guindi, I. Gordon, and O. El Daif, "Influence of Periodic Surface Nanopatterning Profiles on Series Resistance in Thin-Film Crystalline Silicon Heterojunction Solar Cells," IEEE Journal of Photovoltaics, **5**(5), 1319-1324 (2015).
19. P. Campbell, and M. A. Green, "High performance light trapping textures for monocrystalline silicon solar cells," Solar Energy Materials and Solar Cells **65**, 369–375 (2001).
20. G. A. Landis, "Cross-grooved solar cell," U.S. patent number 4,608,451 (1986).
21. G. A. Landis, "Thin, light-trapping silicon solar cells for space," Conference Record of the Twentieth IEEE Photovoltaic Specialists Conference, doi:10.1109/pvsc.1988.105794 (1988).
22. J. Thorstensen, S. E. Foss, and J. Gjessing, "Light-trapping properties of patch textures created using laser assisted texturing," Prog. Photovolt: Res. Appl. **22**, 993–1000 (2014).
23. Sentaurus TCAD, https://www.synopsys.com/silicon/tcad.html.
24. "PV-Lighthouse," www.pvlighthouse.com.au
25. U. Rau, U. W. Paetzold, and T. Kirchartz, "Thermodynamics of light management in photovoltaic devices," Phys. Rev. B **90**, 035211 (2014).
26. M. Smeets, K. Bittkau, F. Lentz, A. Richter, K. Ding, R. Carius, U. Rau and U. W. Paetzold, "Post passivation light trapping back contacts for silicon heterojunction solar cells," Nanoscale **8**, 18726 (2016).
27. Z. Holman, M. Filipic, A. Descoeudres, S. De Wolf, F. Smole, M. Topic, and C. Ballif, "Infrared light management in high-efficiency silicon heterojunction and rear-passivated solar cells," Journal of Applied Physics **113**, 013107 (2013).